

A study of the sensitivity and decomposition of 1,3,5-trinitro-2-oxo-1,3,5-triazacyclo-hexane

H. Östmark *, H. Bergman, K. Ekvall, A. Langlet

National Defence Research Establishment, S-172 90 Stockholm, Sweden

Received 25 August 1994; accepted 16 February 1995

Abstract

The thermal decomposition and thermal stability of 1,3,5-trinitro-2-oxo-1,3,5-triazacyclo-hexane (keto-RDX or K-6) was studied. The keto-RDX synthesis is described, mass spectra (electron impact (70 eV) and chemical ionization) similar to RDX spectra registered under identical conditions are presented, and mass spectroscopy fragmentation paths are proposed. The LI-MS (laser induced/mass spectroscopic) results imply that the first step in the decomposition of keto-RDX is the elimination of NO_2 or HONO and subsequent breakdown of the triazacyclohexane ring. The thermal stability, activation energy ($E_a = 140 \text{ kJ mol}^{-1}$), and frequency factor ($K_0 = 9 \times 10^9 \text{ s}^{-1}$) in the temperature interval 90–120°C were measured using chemiluminescence (NO detection only). The activation energy was also determined from DSC data using the ASTM method E 698–79, and was found to be 280 kJ mol^{-1} with a frequency factor of $7.0 \times 10^{29} \text{ s}^{-1}$ in the temperature interval 175–200°C. Microcalorimetry, drop-weight test, friction test, and ignition temperature (Wood's metal bath) measurements were also conducted. Quantum mechanical calculations (semi-empirical MNDO method with PM3 set at the unrestricted Hartree–Fock level) were conducted to correlate the sensitivity and thermal decomposition with those of RDX. No significant differences in bond-breaking energies for RDX and keto-RDX were found. Conclusions drawn from the experiments are that the decomposition of keto-RDX is auto-catalytic, and that the sensitivity of keto-RDX is not connected with the initial bond-breaking step. More than one method for measuring the risk involved in handling an explosive is necessary since the sensitivity depends on different stages in the decomposition.

Keywords: High explosives; Ignition; K-6 decomposition; Keto-RDX; Laser; Mass spectroscopy; Sensitivity

* Corresponding author.

1. Introduction

RDX is one of the most commonly used high explosives. Thus, a great deal of sensitivity data on RDX has been published, and its thermal decomposition path has been widely examined [1–6]. None of the decomposition studies, however, are conclusive, and no agreement on any single decomposition path has been reached. RDX could well have a thermal decomposition following many different paths. In order to better understand how the sensitivity and the decomposition path is related to the molecular structure, and especially how the sensitivity changes with the introduction of another functional group, we have synthesized a substance, keto-RDX (1,3,5-trinitro-2-oxo-1,3,5-triazacyclohexane), which is very similar to RDX, differing only in the incorporation of a carbonyl group into the six-membered ring. We then measured the sensitivity and studied the thermal decomposition of keto-RDX and tried to correlate these results with those of RDX. Data from the following tests and studies are presented in this paper: drop-weight test, friction test, chemiluminescence, DSC, temperature of ignition test according to Wood's metal bath, microcalorimetry, mass spectra, and LI/MS (laser ignition mass spectroscopy). Semi-empirical quantum mechanical (QM) calculations of the N–NO₂ bond scission energies for both RDX and keto-RDX were also carried out and compared with the experimental results. Keto-RDX also has an interestingly high density ($\rho = 1.93 \text{ g cm}^{-3}$) [7] which makes it a potentially useful explosive. The idea of correlating the sensitivity with the structure for closely related molecules is not new, but in earlier studies only one or two tests were normally used for the correlation [8–10]. In a study on the thermal sensitivity and decomposition of NTO, a more complete set of tests was used [11]. This set of tests, expanded to include others (drop weight, friction, and microcalorimetry) is the basis for this study of the thermal sensitivity and decomposition of keto-RDX. These tests were also used to measure how the small change in structure in keto-RDX compared to RDX alters the sensitivity and the decomposition.

2. RDX decomposition

One of the purposes of this paper is to compare the decomposition paths of two closely related high explosives, keto-RDX and RDX. To facilitate the interpretation of the keto-RDX decomposition data, a short review of RDX decomposition is given here.

In a very early study, Robertson [12] noted the effect of neighbouring molecules on the decomposition of RDX, and showed that one of the decomposition paths is the transfer of an oxygen atom from the NO₂ group to the CH₂ group. Analysis of gases evolved during decomposition showed the presence of NO, N₂O, N₂, CO, CO₂, CH₂O, and H₂O. Another mechanism was proposed by Rauch [13], in which NO₂ mainly derives from a gas phase decomposition and H₂CO and N₂O arise from a liquid phase decomposition. In addition to the above-mentioned decomposition products, HCOOH, NH₃, and hydroxymethyl formamide have also been observed [14, 15]. This implies that the decomposition mechanism leading to the formation of the pyrolysis products is more complicated than simply a unimolecular decomposition. A collision-free IRMPD (IR multiphoton decomposition) experiment by Zhao et al. [1] showed that the

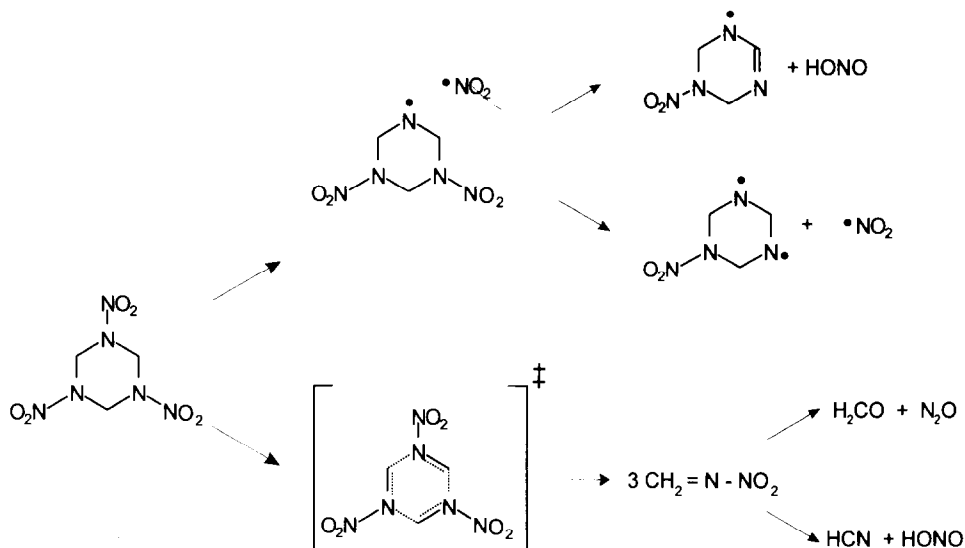


Fig. 1. Decomposition paths for RDX as proposed by Zhao et al. [1].

collision-free decomposition of RDX follows at least two different reaction channels (shown in Fig. 1): via concerted symmetric triple fission and via N–N bond scission.

Mass spectroscopic studies by Bradley et al. [4] and Faber and Srivastava [16] showed that RDX exhibits yet another mode of decomposition, namely one in which the ring is stripped from its NO_2 groups in conjunction with the elimination of one or more hydrogens, forming dihydro-sym-triazin. A closely related mechanism has been proposed by Liebman et al. [17], who proposed the elimination of three HONO or HNO_2 molecules from the ring, forming sym-triazine. The existence of triazine in an RDX decomposition/ignition zone has recently been verified experimentally [18]. The existence of decomposition products which cannot be explained by any of the collision-free decomposition paths indicates that different decomposition mechanisms operate in the gas phases compared to those in condensed phases, which, of course, implies that a larger set of decomposition paths and reaction products has to be used when trying to conclude the sensitivity from the molecular structure. Oyumi and Brill found [15] that at higher pressures, larger fractions of N_2O and CH_2O are present among the decomposition products. They also emphasize the importance of the state of the material in which the reactions take place, and suggest that the decomposition mechanism is linked to the physical processes operating in the material. The slow thermal decomposition processes of both liquid and solid-state RDX exhibit a first-order kinetic deuterium isotope effect (KDIE), indicating that the C–H bond rupture is its rate-controlling mechanistic step [2, 3].

3. Synthesis

Keto-RDX was obtained by a two-step synthesis, see Fig. 2. The six-membered ring was formed by reacting urea, formaldehyde, and *t*-butyl amine [19] giving

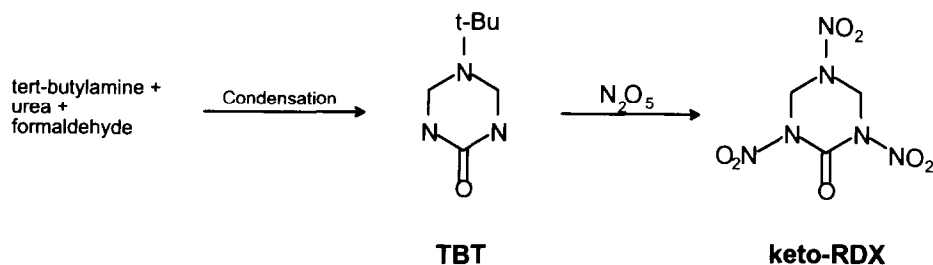


Fig. 2. Synthesis of 1,3,5-trinitro-2-oxo-1,3,5-triazacyclo-hexane (keto-RDX).

2-oxo-5-*tert*-butyltriazole (5-*tert*-butyltriazole, TBT). The intermediate TBT was then nitrated: 26 ml of nitric acid was cooled to -10°C . Keeping the temperature below -5°C , 52 ml of acetic anhydride was added, drop by drop, after which 3 g of TBT was added in small portions, still keeping the temperature below -5°C . The reaction mixture was kept at -2.5°C overnight, and a white precipitate formed. The mixture was allowed to warm up slowly to 5°C after which it was poured over crushed ice, filtered, and the solid precipitate was washed with water. This method yielded 2 g of dry keto-RDX (a 44% yield). The keto-RDX used in this study was purified by several recrystallizations from ethyl acetate.

4. Sensitivity tests

Both the drop-weight sensitivity and the friction sensitivity of keto-RDX were measured. The impact sensitivity was measured with a 2 kg drop-weight BAM apparatus. The results are based on tests on both sides of the 50% probability level using an up-and-down method. The friction sensitivity was measured with a Julius Petri fraction apparatus, using the same technique. The calculations were performed with the ML14 computer code. The results from these calculations can be found in Table 1 where data for RDX are also given for comparison. The results indicate that the sensitivity to friction is about the same for keto-RDX and for RDX, but the sensitivity to impact is significantly higher for keto-RDX. This shows the importance of using more than one of these methods to evaluate the sensitivity and hence the risk involved (see below).

Table 1

Sensitivity data for RDX and keto-RDX, the 50% level with a 95% confidence interval

| Test | RDX | keto-RDX |
|------------------|-------|-------------------|
| Drop-weight test | 38 cm | 7.5 ± 2.5 cm |
| Friction test | 12 kp | 10.8 ± 2.4 kp |

5. Chemiluminescence and DSC

The basic thermal stability of keto-RDX was measured by DSC using a Mettler FP 82. The sample was heated from room temperature with a heating rate of $5^{\circ}\text{C min}^{-1}$. The substance shows a strong exotherm with onset at 188°C and a maximum at 195°C (225°C for RDX). An ocular inspection showed no trace of melting: it appeared as if a gaseous bubble interacted with the solid and formed a liquid phase. The same phenomenon was observed when RDX was tested with the same parameters. Fig. 3 shows a plot of $\ln(\text{heating rate})$ vs. $1/\text{temperature}$ at max isotherm. Using these data and the ASTM method E 698-79, the activation energy (E_a) was measured as 280 kJ mol^{-1} with a frequency factor of $7.0 \times 10^{29} \text{ s}^{-1}$ (temperature interval $175\text{--}200^{\circ}\text{C}$). Compared to RDX, keto-RDX exhibits a larger activation energy, and a very much larger frequency factor. This could possibly explain some of the rather strange sensitivity results obtained.

The chemiluminescence (CL) method was used earlier for decomposition studies at low temperatures [11]. These studies indicated that CL would be useful for determining the kinetic parameters of keto-RDX at low temperatures, and we have used it to study the low-temperature NO development. An apparatus (fully described in Ref. [11] and references cited therein), using the chemical reaction between NO and ozone, was constructed. This method was developed for analysis of propellants, and is not yet fully tested on high explosives. This means that the measurements should be regarded as preliminary, not final, results. Because of this, a comparison with the NO production

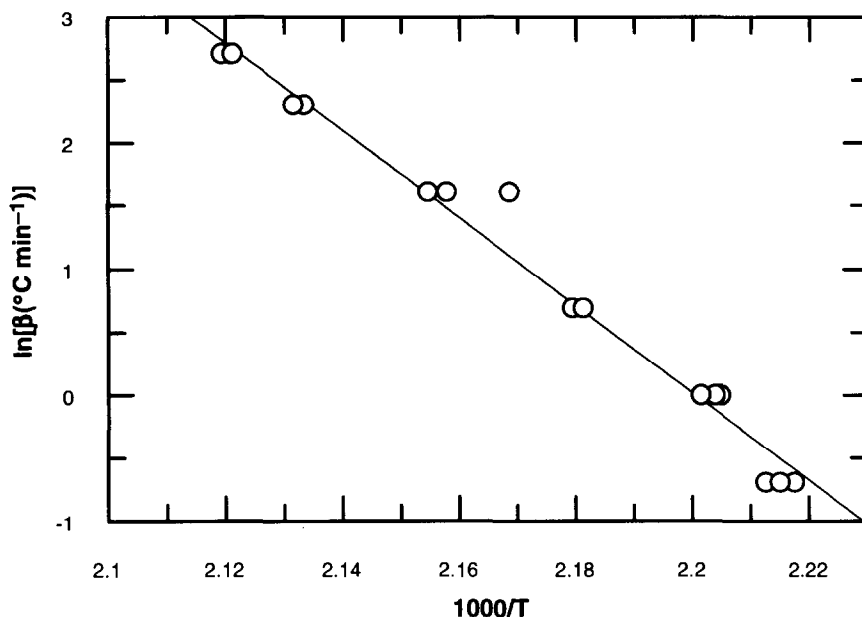


Fig. 3. DSC plot of $\ln(\text{heating rate})$ vs. $1/\text{temperature}$ at max isotherm (ASTM method E 698-79).

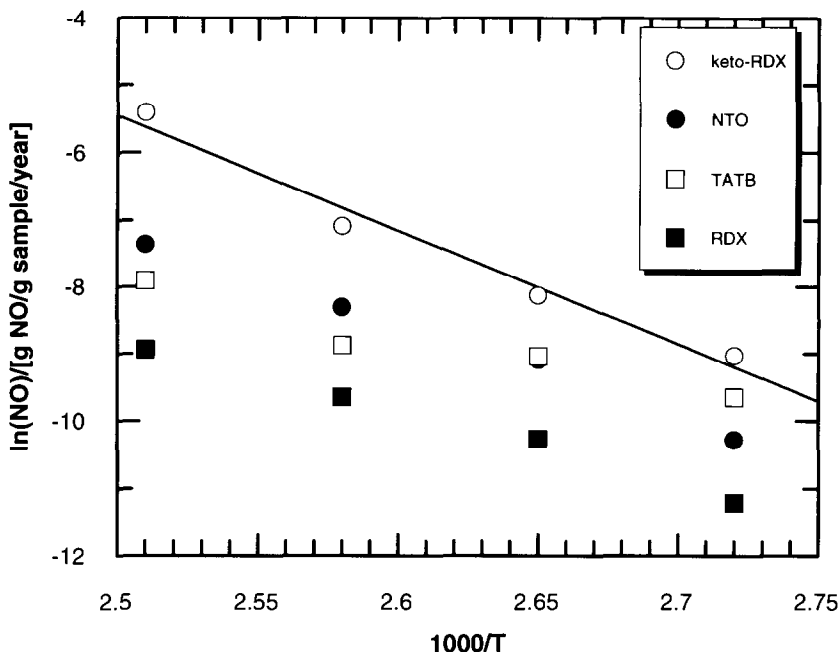


Fig. 4. Production rate of NO vs. temperature for keto-RDX, NTO, TATB, and RDX, measured with chemiluminescence.

for TATB, RDX and NTO is also presented. In Fig. 4, the production rate of NO is shown as a function of temperature for keto-RDX, RDX, TATB, and NTO. A preliminary calculation for keto-RDX in the temperature interval 90–120°C gave us an activation energy (E_a) of 140 kJ mol⁻¹ and a frequency factor (K_0) of 9×10^9 s⁻¹. Fig. 5 shows the production rate of NO at 135°C as a function of time. Here it can clearly be seen that keto-RDX is not stable above 130°C, and will self-heat to a self-sustained decomposition if kept at this temperature.

6. Ignition temperature test

The sensitivity to thermal ignition was measured according to Ref. [20] using Wood's metal bath. The ignition temperature was found to be 170°C. The ignition temperature measured for keto-RDX is relatively low: tetryl tested using the same apparatus under the same conditions gave a temperature of ignition of 207.5°C.

7. Microcalorimetry

An LKB Thermal Activity Monitor equipped with the BOMIC 2277 software was used to monitor the stability of keto-RDX at 65°C. A microcalorimeter measures the sum of

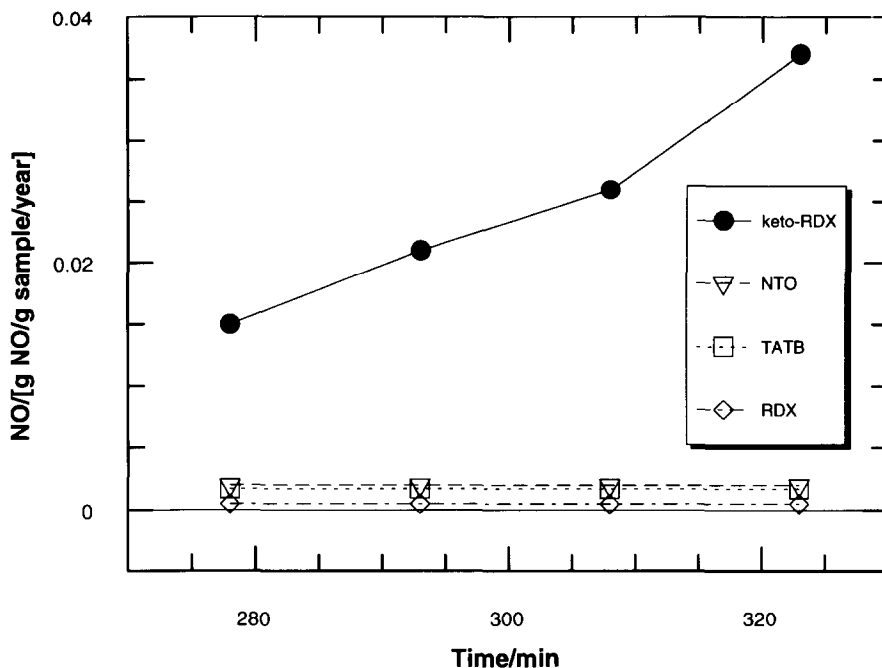


Fig. 5. Production rate of NO vs. time at 135°C for keto-RDX, NTO, TATB, and RDX, measured with chemiluminescence.

all chemical and physical reactions taking place in the sample. The apparatus used is very accurately thermostated, and the accuracy of the apparatus is better than 1 μ W. In Fig. 6 the activity at 65°C over a period of 30 days is shown for keto-RDX and RDX. It can be seen here that the activity is significantly higher for keto-RDX than for RDX.

8. Mass spectroscopy

It has been shown earlier that the thermal fragmentation path of RDX shows similarities to its mass spectral fragmentation [21]. As keto-RDX is very similar to RDX, a mass spectroscopic study is a natural starting point for acquiring new information about the decomposition mechanism. A review of mass spectroscopy on explosives can be found in Ref. [22] which also gives the assignment of the different RDX peaks used in the analysis of the keto-RDX spectra.

The mass spectroscopic study was conducted on a JEOL 300D double-focusing magnetic sector instrument equipped with a PC-based computer system with Technivent Vector/2 software for data analysis. All mass spectra were acquired using the solid sample inlet with a heating rate of about 50°C min⁻¹. Electron impact (EI), 20 and 70 eV, as well as chemical ionization (CI) spectra were acquired. The CI spectra were obtained using methane as the reagent gas. The mass spectra of RDX were registered

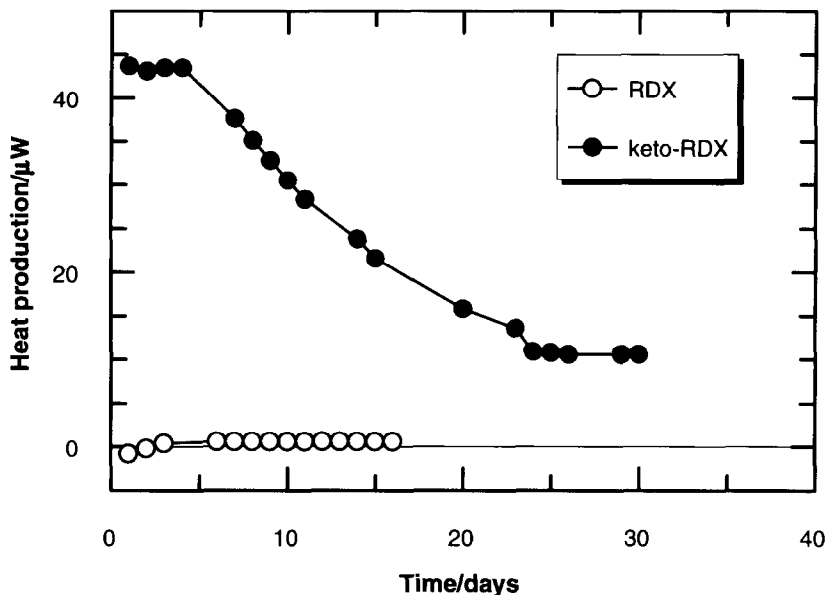


Fig. 6. Heat production vs. time at 65°C for keto-RDX, measured with microcalorimetry.

for comparison and, if possible, to correlate the fragmentation paths of RDX and keto-RDX. In Fig. 7, the mass spectra of keto-RDX and RDX are shown (EI at 70 eV). This figure also shows proposed assignments for some of the peaks. Mass spectra for TBT (5-*tert*-butyl-triazone), the keto-RDX intermediate $C_7H_{15}N_3O$, were also acquired.

The keto-RDX mass spectrum obtained at 70 eV is largely similar to the RDX spectrum, with some notable differences. In the mass spectrum for keto-RDX, the m/z 56 peak is much more intense than it is for RDX, due to additional breakdown products from the ring ($OCNCH_2$). Another slight difference is that in the keto-RDX spectrum, m/z 43, 44, 45, and 47 are stronger compared to those for RDX. The peaks m/z 148 and 120 in the RDX spectrum are explained by Yinon [22], and applying this line of reasoning to the decomposition of keto-RDX, see Scheme A in Fig. 8, the first step would be a $CONNO_2$ elimination which indicates that the keto group makes it easier to extract fragments from the ring. (There are no m/z 134 and 162 peaks which would point to a CH_2NNO_2 extraction.) Another interesting feature of the keto-RDX mass spectrum is the peak at m/z 189 which indicates an HNO_2 (possibly $H + NO_2$) elimination, Scheme B in Fig. 8. This has not been observed for RDX. The strong peak at m/z 130 in the keto-RDX spectrum is still to be explained.

As can be seen in Fig. 7, both keto-RDX and RDX exhibit a molecular peak in the electron impact spectra, even at 70 eV. This observation combined with the ones mentioned above indicates that keto-RDX and RDX have similar mass decomposition paths (at least to some extent) and that the molecular sensitivity is approximately equal.

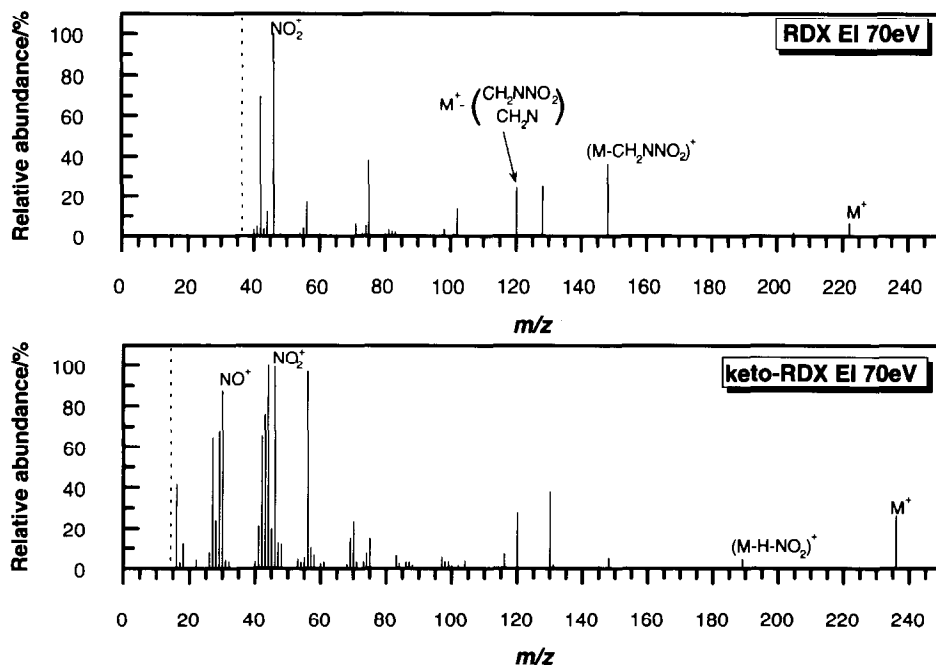
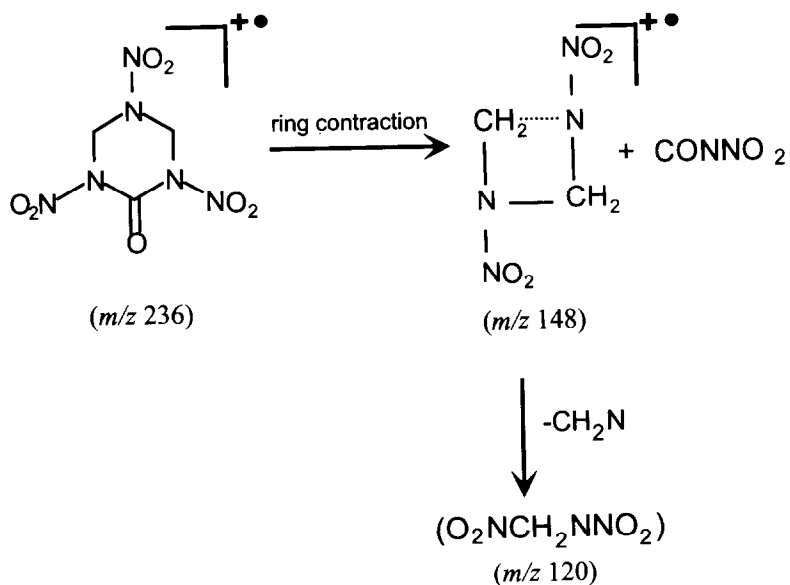


Fig. 7. Mass spectra for RDX and keto-RDX (EI 70 eV).

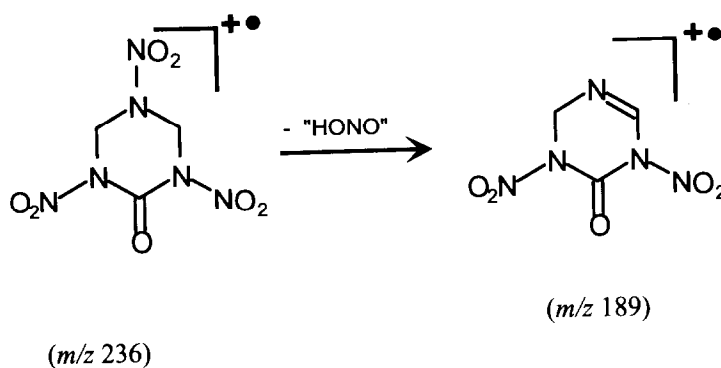
The CI spectrum for keto-RDX (shown in Fig. 9 with an RDX spectrum for comparison) has large similarities with the RDX spectrum in that $(M + H)^+$, $(M + NO)^+$, $(CH_2NNO_2 + H)^+$ and $(CH_2NNO_2 + NO)^+$ can all be found. For keto-RDX, however, no $(M + HCH_2NNO_2)^+$ ion (which is the strongest peak for RDX) can be observed; instead $(OCNNO_2 + H)^+$ and $(OCNNO_2 + NO)^+$ ions are found, and also two unidentified strong peaks at m/z 130 and 204. The interpretation of the mass spectra is based on the RDX assignments of Yinon [22].

9. LI/MS

In order to get a better understanding of the pure thermal decomposition of keto-RDX, the laser-induced mass spectrometry (LI/MS) method [18] was used. This method cannot distinguish between reactions taking place in different interaction phases, since the capillary is placed in the ignition zone and collects products from all participating phases. It is also hard to distinguish decomposition taking place in the decomposition zone from fragmentation occurring in the mass spectrometer [18]. However, this method can give information on which reactions are taking place in the decomposition/reaction zone. The experimental set-up consists of an explosive chamber, a 180 W continuous-wave carbon dioxide laser (Edinburgh PL6) used to heat the sample, thus starting decomposition/ignition of the high explosive, and a mass



Scheme A



Scheme B

Fig. 8. Proposed mass spectroscopic fragmentation paths.

spectrometer (JEOL 300D double-focusing magnetic sector instrument of a Finnigan OWA 1020 quadrupole instrument). As an interface between the reaction chamber and the mass spectrometer, a nearly chemically inert fused-silica capillary was used. Use of a capillary also enabled the application of increased pressure in the explosive chamber,

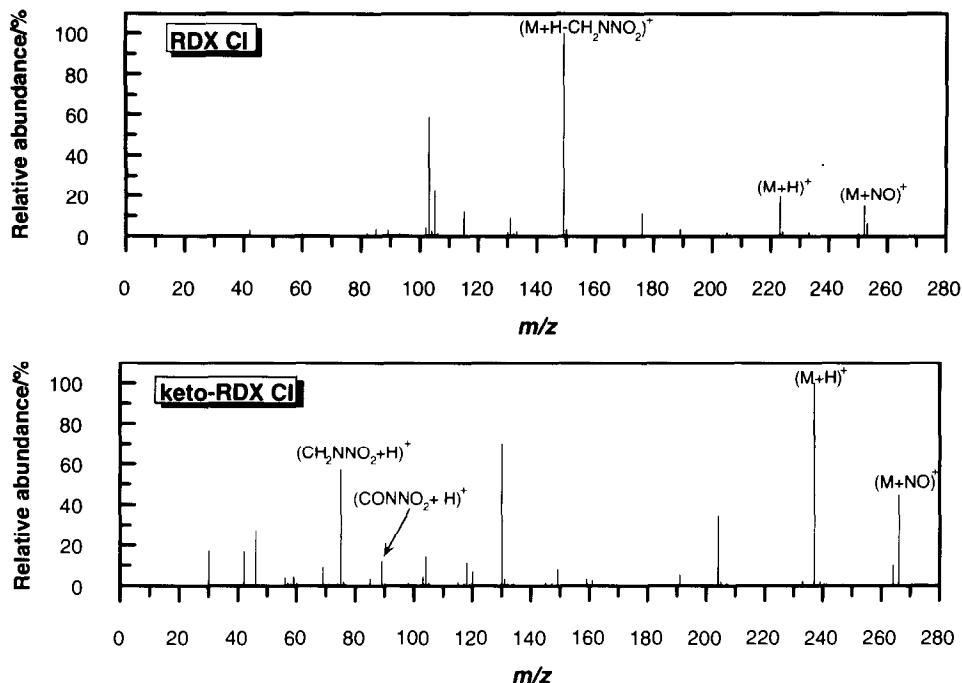


Fig. 9. CI mass spectra for RDX and keto-RDX (methane).

up to 2.5 MPa. A complete description of the laser ignition technique, and how to combine it with different spectroscopic techniques, can be found in Refs. [18, 23–25].

The LI/MS spectra were acquired in a helium atmosphere (0.4 MPa). The decomposition was started by a laser pulse with a pulse width of 4 ms and a power in the interval 25–40 W. The LI/MS method produces a lot of data in a short time, and only a small part of it can be presented here. A compilation of these measurements can be found in Table 2, which shows the most important “thermal” fragments in the laser-induced decomposition zone, and their probable assignments. In the column labelled “strength”, relative measurements of the peak intensity are given, where 1 denotes the most intense peaks and 4 denotes the weakest. Some general observations can be made. It was harder to fine-tune the necessary laser power for acquiring an informative mass spectrum for keto-RDX than for RDX. In most cases, only m/z 44, 30, 46, 32, 29 were found, indicating a complete decomposition. This shows that keto-RDX is more sensitive to pure heat stimuli than RDX.

An interesting observation is that keto-RDX gives more fragments with higher mass than RDX [18]. In the sub-ignition zone of RDX, we could not detect any significant mass peaks larger than m/z 70 (some heavier peaks were detected but only in very small amounts). The existence of several decomposition reaction products with high m/z indicates that concerted symmetric triple fission is less important for keto-RDX than for RDX. Based on this fact and the observations commented on in Table 2, a probable

Table 2
Keto-RDX decomposition peaks and possible assignments

| <i>m/z</i> | Assignment | Strength | Comments |
|-------------|---|----------|---|
| 18 | H ₂ O | 2 | |
| | CN | 2 | |
| 27 | HCN | 2–3 | Increases with laser power |
| 28 | N ₂ , CO | 1 | |
| 29/30 | H ₂ CO | 1 | |
| 30 | (NO) | 1 | Arises mainly from NO + NO ₂ + N ₂ O + H ₂ CO |
| 32 | O ₂ | 1 | A lot of O ₂ is produced during the decomposition of keto-RDX: this is not seen in the decomposition of RDX [18] |
| 40 | | 3 | |
| 41 | | 3 | |
| 42 | N(CH ₂)N, (CH ₂) ₂ N, C(O)N? | 1 | Ring fragments |
| 43 | NCOH, OCNH | 1 | |
| 44 | N ₂ O, CO ₂ | 1 | |
| 45 | H ₂ NCHO? | 2 | |
| 46 | NO ₂ | 1–3 | Strongly dependent on the laser power!! |
| 47 | HNO ₂ | 2–3 | Indicates an HONO elimination |
| 55 | (CO)N(CH) | 4 | Ring fragments |
| 56 | (CO)N(CH ₂), N(CO)N | 3 | Ring fragments |
| 57 | | 3 | |
| 60 | NNO ₂ | 3 | |
| 61/60/46/45 | CH ₃ NO ₂ (nitromethane) | 2 | |
| 61 | HNNO ₂ ? | 2 | |
| 69 | | 3 | |
| 70 | Oxadiazole | 2 | Ref. [34] |
| 71 | | | |
| 73 | | | |
| 75 | | | |
| 81/54 | Triazine | 3 | For RDX, triazine is an indication of a solid-phase decomposition [17] by repeated HONO elimination |
| 87 | CHNNO ₂ CH ₂ | 4 | |
| 88 | (NO ₂)HCO, CH ₂ NNO ₂ CH ₂ | 2 | |
| 89 | | 2 | Highest mass having an intense peak |
| 120 | O ₂ NCH ₂ NNO ₂ ? | 4 | Only visible at low laser power |
| 128 | CHN(CO)NNO ₂ CH | 4 | Decreases with increasing laser power. |
| 205 | ? | 4 | |

decomposition path is the elimination of NO₂ followed by a breakdown of the ring and/or the elimination of HONO followed by a breakdown of the ring, see Fig. 10.

10. Quantum mechanical calculations

For the semi-empirical calculations, the MOPAC 6.0 computer program [26] was used with the MNDO (modified neglect of diatomic overlap) formalism [27] using the PM3

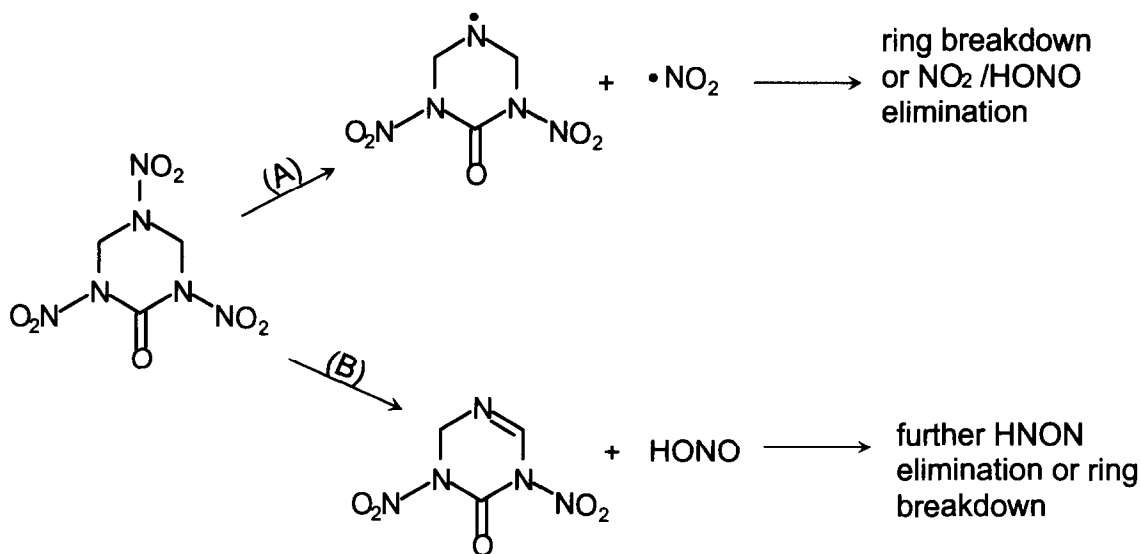


Fig. 10. Proposed thermal decomposition paths for keto-RDX.

parameter set [28, 29] at the unrestricted Hartree–Fock (UHF) level of theory. The MNDO/PM3 combination was shown by Akutsu et al. to give good results for nitramines, nitro aliphates, and nitro aromates [30–32]. RDX can have C_{3v} , C_s , and C_1 molecular symmetry, and keto-RDX can have C_s or C_1 symmetry. In the calculations presented here, we have used the conformation with the highest symmetry (C_{3v} for RDX and C_s for keto-RDX). In a more extensive QM study, all molecular conformations have, of course, to be considered. As already noted, RDX and, possibly, keto-RDX have multiple decomposition paths, of which only two, and then only the first step, will be considered in this QM study, namely N–N bond fission and concerted symmetric triple fission. Because of the complex transition state, the HONO elimination is not considered here.

The potential energy surface for the uni-molecular bond scission of RDX and keto-RDX (N–N bond) was generated by fixing the N–N bond and then fully optimizing the geometry in a number of steps around the equilibrium value. The bond scission energy, ΔE^* , was found to be 22 kcal mol⁻¹ for RDX. The same calculations were performed for the two types of (non-equivalent) N–N bonds in keto-RDX, with the following bond scission energies: $\Delta H_{\text{bond1}} = 26.4$ kcal mol⁻¹ and $\Delta H_{\text{bond2}} = 21.5$ kcal mol⁻¹, respectively. The bond scission energies of the N–NO₂ bond in RDX is $\Delta H_{\text{bond}} = 22$ kcal mol⁻¹ and for keto-RDX, $\Delta H_{\text{bond1}} = 26.4$ kcal mol⁻¹ and $\Delta H_{\text{bond2}} = 21.5$ kcal mol⁻¹, respectively. The concerted symmetric triple fission energies were 68.2 kcal mol⁻¹ for RDX and 67.1 kcal mol⁻¹ for keto-RDX. The QM calculations are summarized in Fig. 11. Clearly the result of this study is that no significant difference in the bond-breaking energies for RDX and keto-RDX exists (at this level of theory).

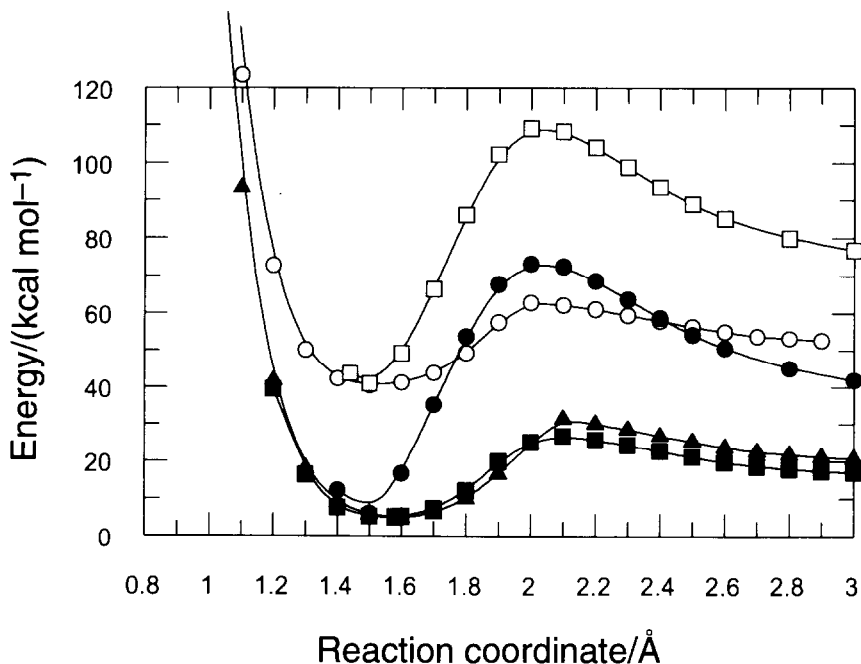


Fig. 11. Potential energy surface for the unimolecular bond scission ($\text{N}-\text{NO}_2$) and for the concerted symmetric triple fission for RDX (\square , triple fission; \circ , NO_2 elimination) and keto-RDX (\bullet , triple fission; \blacktriangle , 1- NO_2 elimination; \blacksquare , 5- NO_2 elimination).

Using semi-empirical methods for calculating absolute heat of reaction or heat of formation in a reaction involving either bond breaking or bond formation, normally gives, to some degree, questionable results. However, when one is only interested in comparing different reaction channels, or when studying closely related molecules, reasonable results may be obtained [33]. We will try to verify these results through ab initio quantum mechanical calculations. In these studies the geometry of the transition states will also be calculated.

11. Discussion and conclusions

Keto-RDX and RDX have very similar mass decomposition paths, and keto-RDX can therefore be used as a model substance when attempting to correlate structure with sensitivity. This study on keto-RDX will be followed by a similar study on difluoro-RDX, in order to achieve a more extensive understanding of the correlation between structure and sensitivity.

Both keto-RDX and RDX exhibit molecular peaks of approximately the same magnitude in the EI spectra at 70 eV, which indicates that the molecular sensitivity is approximately the same for the two substances.

Keto-RDX is found to be more sensitive to impact than RDX, but the sensitivity to friction is approximately equal.

We can clearly see from the CL and DSC measurements that keto-RDX is much more thermally unstable than RDX. The reaction at 135°C in the CL measurements may be caused by auto-catalysis.

The existence of several decomposition reaction products with high m/z indicates that concerted symmetric triple fission is less important for keto-RDX than for RDX. A probable decomposition path is the elimination of NO_2 followed by a breakdown of the ring and/or the elimination of HNON followed by a breakdown of the ring.

QM calculations show that no significant difference in the bond-breaking energies for RDX and keto-RDX exists (at the MNDO/PM3 level of theory). This is contradictory to the large difference in thermal sensitivity. The interpretation may be that the sensitivity of keto-RDX is not determined by the initial decomposition but by reactions occurring later, which may be auto-catalytic.

The results of this study clearly show that the sensitivity of an energetic molecule is a complex issue which may depend on a number of variables. The conclusion we draw from this is that a substance may have different types of sensitivity depending on stimulus input, and that therefore more than one test method must be used in order to fully describe the sensitivity of the substance, and thus assess the risk involved in its handling.

References

- [1] X. Zhao, E.J. Hints and Y.T. Lee, *J. Chem. Phys.*, 88 (1988) 801–810.
- [2] S.L. Rogers, M.B. Coolidge, W.J. Lauerdale and S.A. Shackelford, *Thermochim. Acta*, 177 (1991) 151–168.
- [3] S. Bulusu, D.I. Weinstein, J.R. Autera and R.W. Velicky, *J. Phys. Chem.*, 90 (1986) 4121.
- [4] J.N. Bradley, A.K. Butler, W.D. Capey and J.R. Gilbert, *J. Chem. Soc. Trans. Faraday Soc.*, 73 (1977) 1789.
- [5] R. Behrens, Jr. and S. Bulusu, *J. Phys. Chem.*, 96 (1992) 8891.
- [6] R. Behrens, Jr. and S. Bulusu, *J. Phys. Chem.*, 96 (1992) 8877.
- [7] R. Gilardi, J.L. Flippen-Anderson and C. George, *Acta Crystallogr. Sect. C*, 46 (1990) 706.
- [8] C.B. Storm, J.R. Steine and J.F. Kramer, in S.N. Bulusu (Ed.), *Chemistry and Physics of Energetic Materials*, Kluwer Academic Publishers, Dordrecht, 1990, Nato ASI Series: Serie C-Vol. 309.
- [9] C.B. Storm, R.R. Ryan, J.P. Ritchie, J.H. Hall and S.M. Bachrach, *J. Phys. Chem.*, 93 (1989) 1000–1007.
- [10] T.B. Brill, in S.N. Bulusu (Ed.), *Chemistry and Physics of Energetic Materials*, Kluwer Academic Publishers, Dordrecht, 1990, Nato ASI Series: Serie C-Vol. 309.
- [11] H. Östmark, H. Bergman and G. Åqvist, *Thermochim. Acta*, 213 (1993) 165.
- [12] A.J.B. Robertson, *Trans. Faraday Soc.*, 45 (1949) 85.
- [13] F.C. Rauch and A.J. Fanelli, *J. Phys. Chem.*, 73 (1969) 1604.
- [14] J.D. Cosgrove and A.J. Owen, *Combust. Flame*, 22 (1974) 13.
- [15] Y. Oyumi and T.B. Brill, *Combust. Flame*, 62 (1985) 213.
- [16] M. Faber and R.D. Srivastava, *Chem. Phys. Lett.*, 64 (1979) 307.
- [17] S.A. Liebman, A.P. Snyder, J.H. Kremer, D.J. Reutter, M.A. Schroeder and R.A. Fiefer, *J. Anal. Appl. Pyrolysis*, 12 (1987) 83.
- [18] H. Östmark, H. Bergman and K. Ekvall, *J. Anal. Appl. Pyrolysis*, 24 (1992) 163.
- [19] R.D. Lear and R. McGuire, *Energy Technol. Rev.*, March (1988) 22.
- [20] Sprängämnesinspektionen, TESTBATTERI/EX (1986).

- [21] J. Stals, *Trans. Faraday Soc.*, 6 (1971) 67.
- [22] J. Yinon, *Mass Spectrom. Rev.*, 1 (1982) 257.
- [23] H. Östmark and N. Roman, *J. Appl. Phys.*, 73 (1993) 1993.
- [24] H. Östmark and R. Gräns, *J. Energetic Mater.*, 8 (1990) 308.
- [25] H. Nilsson and H. Östmark, in *Ninth Symposium (International) on Detonation*, Office of Naval Research ONR 113291–7, Portland, Oregon, 1989, Vol. II, pp. 1151–1161.
- [26] J.J.P. Stewart, *J. Computer-Aided Molecular Design*, 4 (1990) 1.
- [27] J.J.S. Dewar and W. Thiel, *J. Am. Chem. Soc.*, 99 (1977) 4899.
- [28] J.J.P. Stewart, *J. Comp. Chem.*, 10 (1989) 209–220.
- [29] J.J.P. Stewart, *J. Comp. Chem.*, 10 (1989) 221.
- [30] Y. Akutsu, J. Takayama, M. Tamura and T. Yoshida, *J. Energetic Mater.*, 10 (1992) 173.
- [31] Y. Akutsu and S. Tahara, *J. Energetic Mater.*, 9 (1991) 161.
- [32] Y. Akutsu, R. Che and S. Tahara, *J. Energetic Mater.*, 11 (1993) 195.
- [33] Y. Shi and S.M. Senkan, *J. Phys. Chem.*, 95 (1991) 5181.
- [34] T.L. Boggs, *Progr. Astronaut. Aeronaut.*, 90 (1994) 177.